Wavelet analysis of blood flow singularities by using ultrasound data

By Philippe May

1. Motivation and objectives

The effects of blood flow turbulence are of great clinical importance in both medical and surgical areas. For example, several biological research fields have focused on the role played by turbulence on cell and tissue behavior, It is now well established that the transition to turbulence is expected to be dependent on flow pulsatility and on the nature of the arterial wall. There is evidence suggesting that the effect of pulsatility on transition to flow turbulence is common in a wide variety of arterial flows and several studies support this view (Winter 1984; Ku 1997). In addition, the presence of an intra-arterial singularity such as a stenosis, an aneurysm or a thrombosis is known to greatly increase the probability of transition to turbulence downstream of the singularity.

In the study of vascular physiology, Nerem (1993) demonstrated the decrease of cell proliferation and the alteration of cell morphology when vascular endothelium is exposed to laminar shear stress. This laminar blood flow induces endothelial cells to exhibit a non-reactive phenotype. Davies *et al.* (2001) demonstrated *in vitro* that disturbed flows induce greater variability of gene expression from cell to cell than do undisturbed laminar flows. Microgravity experiments have shown that the low-turbulence culture environment (simulated with the NASA Bioreactor) promotes the formation of large, three-dimensional cell clusters and has provided insight into better understanding of normal and cancerous tissue development (Gao *et al.* 1997; Radin *et al.* 2001). Because high turbulence levels can damage cells (Davies *et al.* 1986), the determination and control of the turbulence levels that optimize expression of differentiated function and tissue development is of great importance.

At a larger vascular scale, the location of atherosclerotic lesions near branches, bifurcations, and curvatures of arteries has long been identified. For instance, Ku *et al.* (1985) found a strong correlation between flow disturbances and arterial susceptibility to the development of atherosclerosis plaque. Tsao *et al.* (1996) demonstrated that the effects of flow in inhibiting atherogenesis appear to be mediated in part by the endothelium-derived nitric oxide (NO). Bluestein *et al.* (1999, 2000) demonstrated the correlation between the generation of shed vortices downstream of an arterial singularity, and with both the local platelet deposition and the free emboli of platelet aggregates. These local hemodynamics are widely believed to impact vascular diseases, from the development and progression of vascular lesions to the production of the thromboemboli and the cholesterolemboli that cause heart attacks and strokes.

For all of these reasons, but not limited to, the analysis of the intra-vascular blood flow behavior requires a much better understanding under simulated and physiological conditions, with the needed development of devices and tools to accurately determine the turbulence levels of blood flow in real-time.

For this purpose, an ideal system to study is the generation of turbulence downstream of a singularity: the generated turbulence is strong and, has in many various fields, important implications of increasing the accuracy of real-time detection procedures.

In biology and medicine there are usually differences amongst individuals when studying the time evolution of physiological parameters of a non-pathological human group. Therefore, the use of dimensionless numbers to describe biological flow disturbances is of higher relevance in conducting biological research flow studies. Since a Reynolds' number (Re) is usually defined for steady flow through rigid tubes, it may not reflect the actual fluid behavior of intra-vascular pulsatile flow. The Womersley' number (Wo) which includes the pulsatile and frequency behavior of the flow is a better parameter, but has the same limitation as Re. Because biological fluid dynamics invariably involves the interaction of visco-elastic and active tissue with viscous incompressible non-Newtonian fluid, this interaction can not be neglected in biological fluid mechanics research and computation of biological models, as pointed out by Peskin *et al.* (1995) with the immersed boundary method; and considered in their studies by Ye *et al.* (1999).

Since Leonardo Da Vinci's studies of cardiovascular systems by using a simple aortic glass model to simulate flow dynamics (Gharib *et al.* 2002), - 400 years ahead of Osborn Reynolds' famous pipe flow visualization studies -, the real-time detection of blood flow behavior has gained more and more importance. This requires non-invasive and safe vascular imaging techniques of the highest resolution in space and time. Since Schmidt *et al.* (1970), significant advances in ultrasonic flow measurements have been made. Ultrasonics are widely used in both medical and surgical areas (Cloutier *et al.* 1990), and this device demonstrated in fluid mechanics its utility where opaque flow fields preclude the use of optically-based diagnostic tools (Johari *et al.* 1998; Nowak 2002).

When analysing a scientific image, the main goal is to describe it quantitatively. This goal is difficult to achieve without the use of mathematical tools because human interpretation can often be subjective. Recently, there has been increasing interest in the study of scaling behavior in irregular objects: the velocity field of fully developed turbulent flows (Farge *et al.* 1988; Meneveau 1991; Muzy *et al.* 1991; Frisch 1995; Arnéodo *et al.* 1995), financial time-series (Mantegna *et al.* 2000), telecommunication traffic (Abry *et al.* 2002), medical time-series (West 1990), random walks associated with DNA sequences (Arnéodo *et al.* 1996).

Adapting the methodology of Farge (1992); Arnéodo *et al.* (1995), and in order to analyze scaling behavior and singularities in pulsatile blood flows as previously done by May *et al.* (2001a,b, 2002), the goal of this study is to use the wavelet signal processing strategy on bidimensional vascular data:

- In part I, adapting the work of Farge (1992) & later Kailas *et al.* (1999), the basic methodology is outlined to examine the 2D wavelet transform of vascular flow images at various scales, especially when the images indicated the presence of intervals during which the blood flow pattern downstream of the lesion contains shedding vortices. Kailas *et al.* (1999) made this analysis from images taken of a mixing layer (Roshko 1954; Bloor 1964).
- In part II, adapting the work of Arnéodo *et al.* (1995) & Haase (2000), the wavelet transform modulus maxima (WTMM) method is applied on the same data for extracting singularities of the velocity field by analyzing all vertical 1D cross sections of each image (Figure 1).

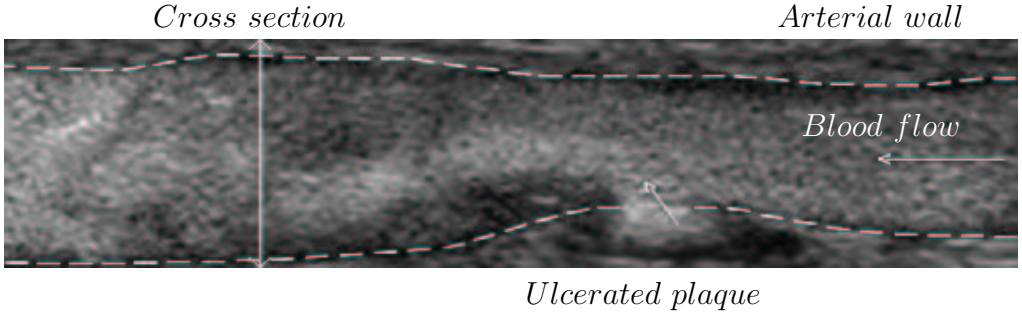

FIGURE 1. Turbulence induced by an ulcerated plaque located in a carotid artery and imaged by Doppler ultrasound (General Electric Corporation, LaConte (2002)).

2. Methods

2.1. *Ultrasound data used*

Ultrasound datasets were recorded upstream and downstream of an ulcerated atherosclerosis plaque located in the human carotid artery (LaConte 2002). The basic variable of the images, $f(x)$ is the grey-scale intensity correlated with the blood flow velocity, and x is the two-dimensional position vector. The images were digitized with 512×128 pixels and 8 bit accuracy providing 256 grey levels of image intensity.

2.2. *The Fourier transform*

The Fourier transform has long been a principle analytical tool in various fields such as linear systems, optics, probability theory, quantum physics, antennas, and signal analysis. This mathematical tool originally was used for analysis of stationary signals and systems. The Fourier transform, with its wide range of applications, like many other mathematical tools, has its limitations. For example, this transformation cannot be applied to non-stationary signals. These signals have different characteristics at different times or space coordinates. The modified version of the Fourier transform, referred to as short-time (or time-variable) Fourier transform, can resolve some of the problems associated with non-stationary signals but does not address all the issues of concern. The Fourier transform is a classical tool for measuring the regularity of a function $f(x)$ by investigating the asymptotic decay of its Fourier transform $\hat{f}(w)$ as $w \to \infty$. However, since all local information is unlocalized by the Fourier transform, the asymptotic decay can only give overall information about singularities within the interval considered.

2.3. *The wavelet transform*

By definition, wavelet analysis acts as a mathematical microscope which allows one to zoom in on the fine structure of a signal, or, alternatively, to reveal large scale structures by zooming out. Therefore, when a signal or a process contains some form of scale invariance or some self-reproducing property under dilatation, wavelets are useful in identifying them. The wavelet transform (WT) of a real valued function f, according to the analysing mother wavelet ψ, is defined as the convolution product of the scaled and shifted mother wavelet ψ with $f(x)$ (Goupillaud *et al.* 1984),

$$T_\psi[f](a,b) = \frac{1}{a}\int_{-\infty}^{+\infty} f(x)\psi(\frac{x-b}{a})dx, \qquad (a,b \in \mathbb{R}, a > 0) \tag{2.1}$$

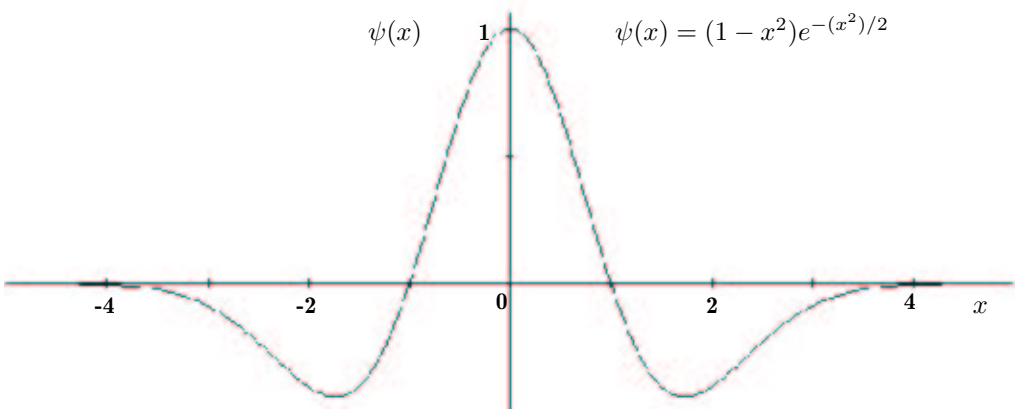

FIGURE 2. The Mexican hat mother wavelet.

The wavelet transform (WT) decomposes a signal $f(x) \in L^2(\mathbb{R})$ hierarchically in terms of elementary components $\psi(\frac{x-b}{a})$, which are obtained from a single mother function $\psi(x)$ by dilatations and translations. Here a denotes the scale parameter and b is the shift parameter. The crucial point is to choose $\psi(x)$ to be well localized both in physical and Fourier space. In contrast to Fourier analysis, the WT does not lose information about the position of transient phenomena and irregular structures. In order to detect singular behavior one has to choose an analyzing wavelet $\psi(x)$ that is orthogonal to polynomials of up to order n. The first n moments of $\psi(x)$ are vanishing (Mallat *et al.* 1992).

$$\int_{-\infty}^{+\infty} x^k \psi(x) dx = 0, \qquad (0 \leq k < n) \tag{2.2}$$

2.4. *The Gaussian functions*

A very common way to build admissible wavelets of arbitrary order n is to successively differentiate a smoothing function. Confining to singularities, a family of real valued wavelets constructed from a Gaussian distribution $\psi_0(x)$ has proven to be very effective and has good scale-space localization,

$$\psi_0(x) = e^{-x^2/2}, \qquad \psi_n(x) = \frac{d^n}{dx^n}\psi_0(x), \qquad (n \in \mathbb{Z}) \tag{2.3}$$

The mother wavelet adopted here is the second derivative of the Gaussian function: the Mexican hat (Figure 2), which was the first function used to computationally detect multiscale edges (Witkin 1983),

$$\psi(x) = (1 - x^2)e^{-(x^2)/2}, \tag{2.4}$$

The wavelet transform is successfully applied to non-stationary signals for analysis and processing and provides new techniques which deserve special attention in the area of fractal analysis and synthesis since they can be used to extract *microscopic* information on their scaling properties. Fractals have a complex geometrical shape and are charac-

terized by a non-integer dimensionality defined as follows: the minimum number N of balls of size ε required to cover the set completely behaves like,

$$N(\varepsilon) \propto \frac{1}{\varepsilon^D}, \qquad (\varepsilon \to 0) \tag{2.5}$$

where D is the $fractal\ dimension$.

In this respect, every point is associated with a singular behavior. Fractals are invariant under a group of self-affine transformations including translations and dilatations which are the basic operations in wavelet theory.

2.5. *Detection of signal singularities*

A standard way of characterizing irregular distributions is to extract *macroscopic* information about the underlying hierarchical structure and to statistically describe the scaling properties using concepts such as the generalized fractal dimensions D and the multifractal spectrum $f(\alpha)$. Wavelet analysis represents a generalization of the standard box-counting technique. It allows the estimation of the entire spectrum of singularities $D(h)$ (h is the Hölder exponent) of fractal distributions as well as functions.

In order to locally characterize the irregularity of an object, one generally uses the notion of Hölder exponent h. This exponent can be seen as a measurement of the strength of the singularity behavior of a given function $f(x)$ around a given point $x = x_0$. It is defined as the greatest exponent h so, that f is *Lipschitz* h at x_0, and x_0 is a singularity called *cusp* with Hölder exponent $h(x_0)$. For example, $f(x) = \sqrt{x}$ has a *cusp* at $x_0 = 0$ with Hölder exponent $h(0) = 1/2$, the Heaviside function has a "jump"at $x_0 = 0$ with $h(0) = 0$. In that sense, the Hölder exponent generalizes the notion $order\ of\ differentiability$ and measures the strength of irregularities in the function or in its derivative. f is said to be *Lipschitz* h at x_0 if and only if there exists a constant C and a polynomial $P(x)$ of order smaller than h so that, for all x in a neighborhood of x_0 (Mallat 1998),

$$|f(x) - P(x - x_0)| \leq C|x - x_0|^h. \tag{2.6}$$

The higher the exponent $h(x_0)$, the more regular the function f. In the case where f is made up of an accumulation of singular behavior (which is the case in a fractal function), the direct estimation of $h(x_0)$ and the estimation of the singularity spectrum $D(h)$ of a singular function f, requires the multifractal formalism (Frisch 1995; Arnéodo *et al.* 1995), which provides a "global"method for estimating this singularity spectrum based on the computation of a partition function. It can be shown (Mallat *et al.* 1992) that for *cusp* singularities, the location of the singularity can be detected, and the related exponent can be recovered from the scaling of the WT along the so-called maxima line, converging towards the singularity. This is a line where the WT reaches local maximum (with respect to the position coordinate). Connecting such local maxima within the continuous wavelet transform "landscape"gives rise to the entire tree of maxima lines. It incorporates the main characteristics of the WT: the ability to reveal the hierarchy of (singular) features, including the scaling behaviour. This Wavelet Transform Modulus Maxima (WTMM) tree has been used for defining the partition function based multifractal formalism,

$$Z(q, a) = \sum_i |T_\psi[f](x_i(a), a)|^q, \tag{2.7}$$

where q are the moments of the measure distributed on the WTMM tree.

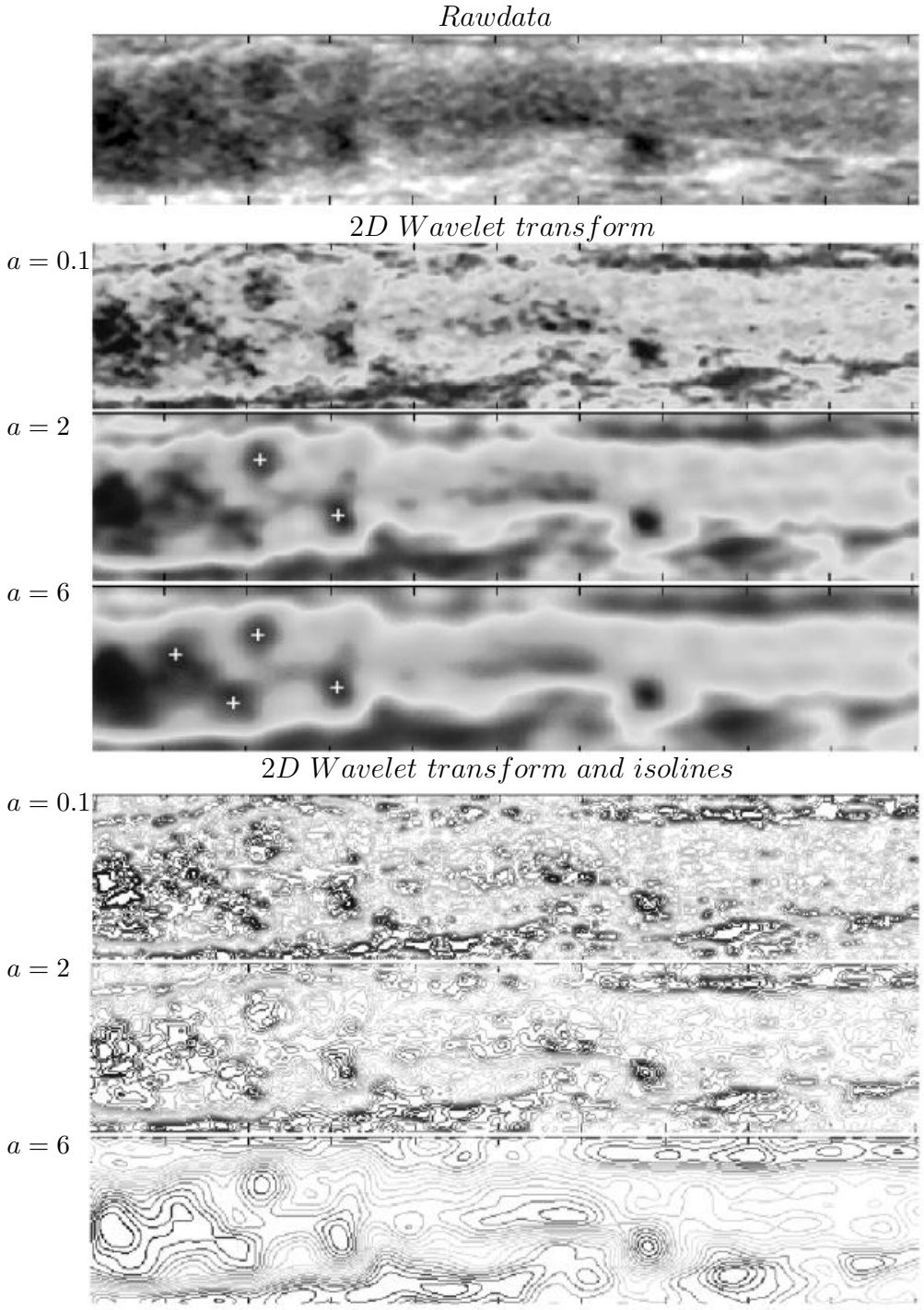

FIGURE 3. Vortex street induced by an ulcerated plaque located in a carotid artery and imaged by Doppler ultrasound (General Electric Corporation, LaConte (2002)).

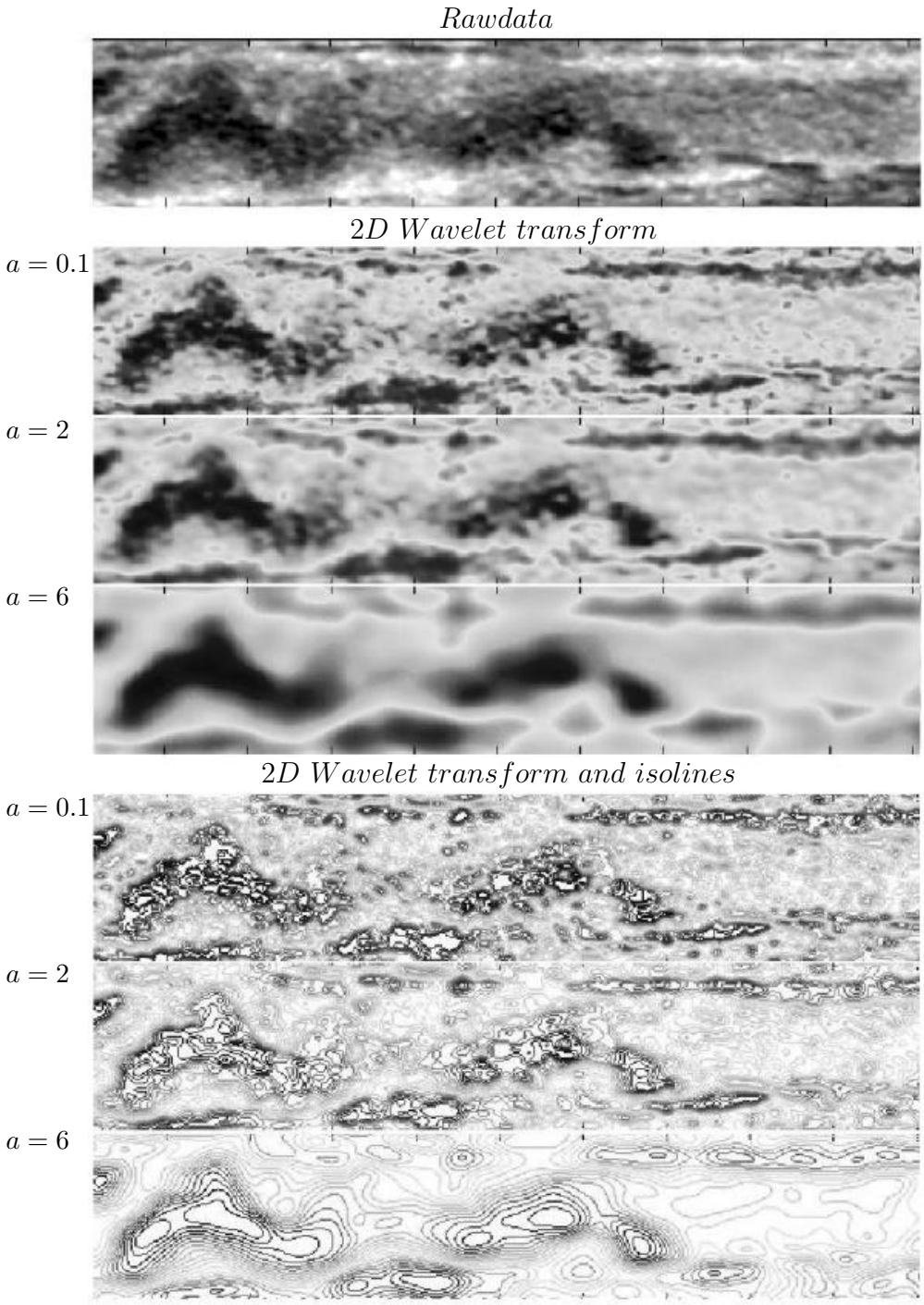

FIGURE 4. Wake induced by an ulcerated plaque located in a carotid artery and imaged by Doppler ultrasound (General Electric Corporation, LaConte (2002)).

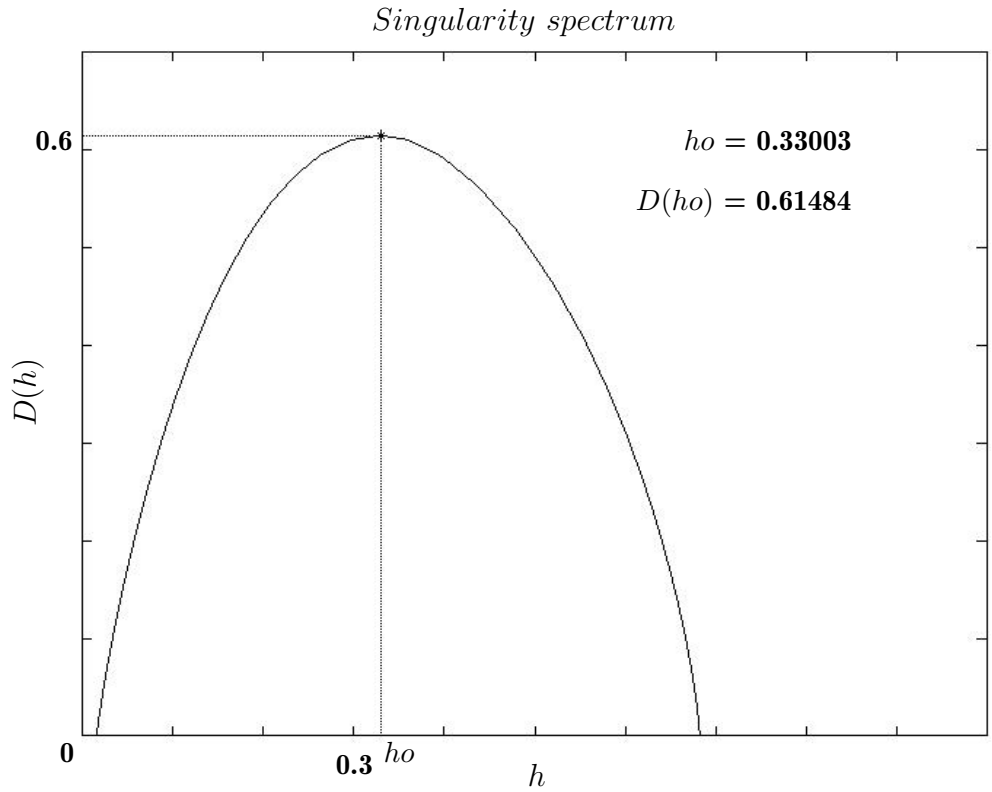

FIGURE 5. Singularity spectrum of a vertical cross section, (analysing wavelet ψ_2).

Arnéodo *et al.* (1995) demonstrated that all the local maxima $x_i(a)$ of $|T_\psi[f](x,a)|$ can be considered as a function of x and proved that, for a large class of fractal functions, $Z(q,a)$ follows a power law scaling

$$Z(q,a) \sim a^{\tau(q)}, \qquad a \to 0^+ \tag{2.8}$$

The $Z(q,a)$ is the partition function of the q-th moment of the measure distributed over the wavelet transform maxima at the scale a considered and the exponents $\tau(q)$ are related to the $D(h)$ singularity spectrum (Figure 5) through the Legendre transform

$$D(h) = min_q(hq - \tau(q)). \tag{2.9}$$

Haase (2000) successfully applied the WTMM method to turbulent data from an axisymetric jet with helium at low temperature (Chabaud *et al.* 1994) previously used to analyze turbulent intermittency. The range of Hölder exponent h was between 0 and 0.8, with the most frequent exponent h found for the maximum of the spectrum close to the classical Kolmogorov value of 1/3.

3. Results

3.1. *First description of the ultrasound data used*

A Doppler ultrasound image of an ulcerated plaque located in the wall of a carotid artery is shown in Figure 1. The velocity blood flow is digitized with a lighter shade of gray scale. The real-time analysis of the blood flow behavior during each heart cycle, indicates the presence of intervals during which the blood flow pattern downstream of the lesion contains shedding of vortices. Upstream of the lesion, the flow is radially uniform except in the boundary layer near the wall of the artery. As reported by Owsley (2000), the flow of the plaque is wave-like with a velocity variation wavelength that can be related, under ideal static lesion symmetry conditions, to the Strouhal vortex shedding rate frequency, $f_s = S(v_p/d_p)(A_p/A_c)^{1.5}$. Here $S = 0.2$ is the Strouhal number ($S = f_s.d_p/v_p$), v_p is the average upstream flow velocity, d_p is the proximal artery diameter, A_p and A_c are the proximal and lesion-constrained artery cross sectional areas respectively (Owsley 2000). In practice, the lesion morphology is neither symmetric nor static in time. For $d_p = 3.18$ mm, using the ranges of values $30 < v_p < 60$ cm/s and $2 < (A_p/A_c) < 9$, the vortex shedding frequencies are ranged between 50 and 1000 Hz (Owsley 2000). This downstream turbulence dissipates blood flow kinematic energy to the artery wall through boundary layer effects and is able to promote morphological changes of the cellular tissue surrounding the artery. Using these velocity values, the estimated Reynolds number in two smooth and rectilinear pipes with a diameter of 3 to 5 mm is respectively $239_{Re_{min}}$ and $795_{Re_{max}}$. With $\rho = 1060\ kg/m^3$ and $\mu = 0.004\ kg/(m.s)$.

In a purely oscillating case, according to Hino *et al.* (1983), the oscillating flow remains stable for $Re < 400$, for $400 < Re < 800$ the flow undergoes a periodically transition between laminar and turbulent states; finally, it becomes fully turbulent for $Re > 800$.

3.2. *Part I: the 2D wavelet transform*

The WT was used on ultrasound images taken at the middle of a heart cycle when the existence of blood flow coherent structures, mostly generated downstream of a singularity, is unambiguous. Figures 3 and 4 depict two different states of the shedding vortices produced and the WT at three different scales (0.1, 2 & 6). In addition, the isolines of each WT were represented to clarify our purpose. At the smallest scale $a = 0.1$, the fine scale structure is apparent and in comparison with the raw data the coherent structures are easily identified. However as a increases we can easily identify, at each scale, the regions of stronger and weaker gradients. In Figure 3 the vortices (white cross) and the connectedness between them are clearly shown for the scales larger than $a = 2$. In Figure 4 the connectedness of the two main wakes are evident in the raw data. Again for scales larger than $a = 2$, a discontinuity is observed between the two main wakes. The same flow characteristics were seen for all the images taken at the middle of a heart cycle. These results demonstrated that the WT captures the profile of the sharp density gradients more clearly than the raw data.

3.3. *Part II: singularity signal analysis in ultrasound images*

The WTMM method was applied to the 512 vertical cross sections of each image (Figure 1) in order to compute the singularity spectrum (Figure 5) of each 1D signal cross section.

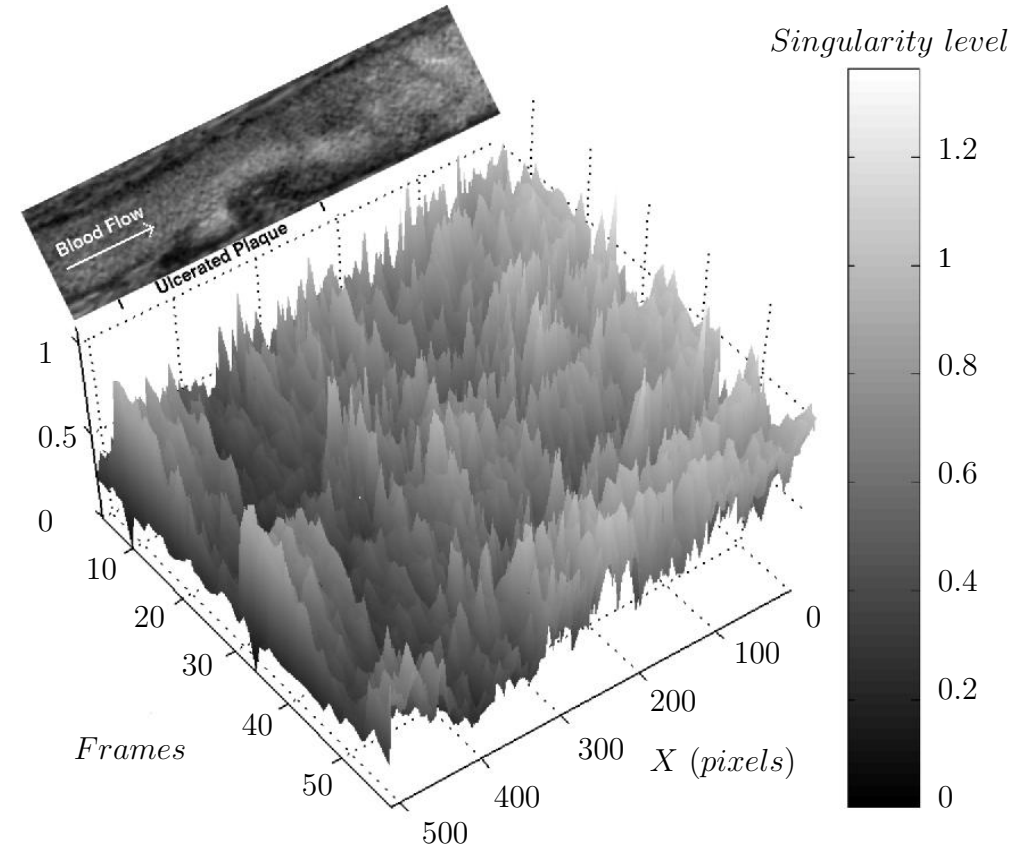

FIGURE 6. 3D representation of the singularity levels calculated for all the frames.

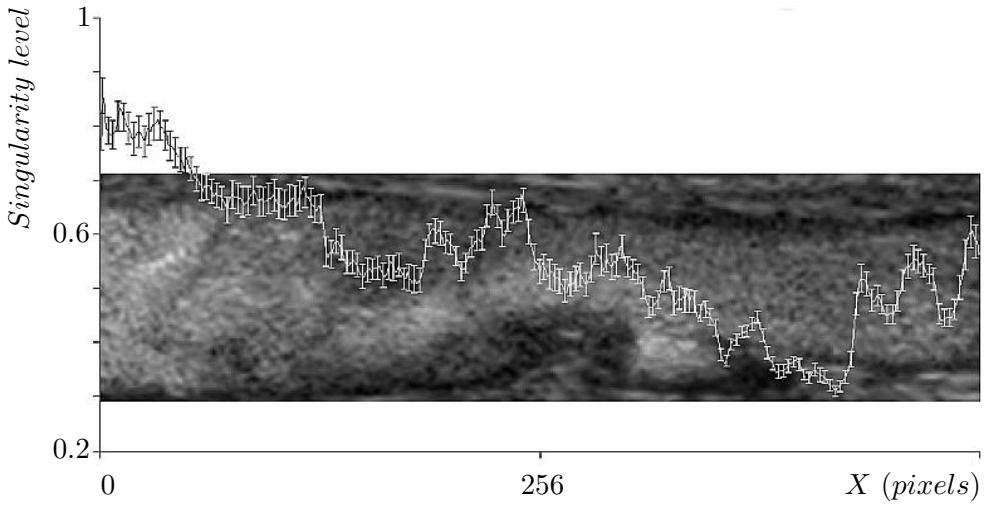

FIGURE 7. Means and SEM of the singularity levels calculated for all the frames.

A numerical code (May *et al.* 2001b)‡ was used to compute the variation of the Hölder exponent h and of $D(h)$. These computations allowed the representation of the singularity level of each 1D signal cross section as a function of the position X and of the time/frame (3D graphical representation of Figure 6). The means of the singularity level of each 1D signal cross section in function of the position X are shown in Figure 7 with an ultrasound frame in the background. As observed by Owsley (2000), after visualizing the ultrasound data, Figure 6 and Figure 7 showed the constant decrease of the singularity level for the upstream region over the plaque for all frames. This singularity decrease is in good comparison with the turbulence decrease of a boundary layer over a two-dimensional bump, experimentally observed by Webster *et al.* (1996).

4. Future plans

The present study has employed a numerical analysis method which is used in other research areas in studying fluid mechanics. In particular, singularity information was extracted from one- and two-dimensional data by this method. This wavelet based method is able to capture the real-time complex biological flows behavior and for instance to evaluate the effect of pharmacological drugs on hemodynamics, and thus its validity should be checked using other flow data behavior taken from simulation and/or experimental biological fluid mechanics. Future work will focus on the validation of this wavelet analysis method with simulation data of biological fluid mechanics.

Acknowledgments

General Electric Corporation is gratefully acknowledged for providing the ultrasound data used in this study. The author wishes to thank Professor David Donoho (Statistics Department, Stanford University) for the wavelet software package "WaveLab". Special thanks to Dr. Y. Dubief for sharing his knowledge of turbulence and for his corrections and helpful comments on the manuscript. I am also thankful to Dr. C.M. White and Dr. J.S. Hur for the helpful corrections and suggestions on the manuscript.

‡ All computations were realized with a numerical code based on a collection of Matlab function files included in the WaveLab 802 package (Pr. David Donoho, Statistics Department, Stanford University).

REFERENCES

Abry, P. & Baraniuk, R. & Flandrin, P. & Riedi, R. & Veitch, D. 2002 Multiscale nature of network traffic. *IEEE Signal Processing Magazine* **19(3)**, 28-46.

Arnéodo, A. & Argoul, F. & Bacry, E. & Elezgaray, J. & Muzy, J.F. 1995 *Ondelettes, Multifractales et Turbulences.* Diderot, Arts et Sciences, Paris, New-York, Amsterdam.

Arnéodo, A. & d'Aubenton-Carafa, Y. & Bacry, E. & Graves, P.V. & Muzy, J.F. & Thermes, C. 1996 Wavelet-based fractal analysis of DNA sequences. *Physica D.* **96**, 291-320.

Bloor, M.S. 1964 The transition to turbulence in the wake of a circular cylinder. *J. Fluid Mech.* **21**, 290.

Bluestein, D. & Gutierrez, C. & Londono, M. & Schoephoerster, R.T. 1999 Vortex Shedding in Steady Flow Through a Model of an Arterial Stenosis and its Relevance to Mural Platelet Deposition. *Annals of Biomedical Engineering.* **27**, 763-773.

Bluestein, D. & Rambod, E. & Gharib, M. 2000 Vortex Shedding as a Mechanism for Free Emboli Formation in Mechanical Heart Valves. *Journal of Biomedical Engineering.* **122**, 125-134.

Brown, G.L. & Roshko, A. 1974 On density effects and large structures in turbulent mixing layers. *J. Fluid Mech.* **64**, 775-816.

Chabaud, B. & Naert, A. & Peinke, J. & Chillà, F. & Castaing, B. & Hebral, B. 1994 Transition toward developed turbulence. *Phys. Rev. Lett.* **73**, 3227-3230.

Cloutier, G. & Lemire, F. & Durand, L.G. & Latour, Y. & Langlois, Y.E. 1990 Computer evaluation of Doppler spectral envelope area in patients having a valvular aortic stenosis. *Ultrasound Med. Biol.* **16(3)**, 247-260.

LaConte, K. 2002 Courtesy of LaConte Kirstin, Global Clinical Marketing Program Manager, *GE Ultrasound*, Milwaukee, WI, October 2002.

Davies, P.F. & Remuzzi, A. & Gordon, E.J. & Dewey, C.F. & Gimbrone, M.A. 1986 Turbulent Fluid Shear Stress Induces Vascular Endothelial Turnover In Vitro. *Proceedings of the National Academy of Sciences.* **83**, 2114-2117.

Davies, P.F. & Shi, C. & Depaola, N. & Helmke, BP. & Polacek, DC. 2001 Hemodynamics and the focal origin of atherosclerosis: a spatial approach to endothelial structure, gene expression, and function. *Ann. N. Y. Acad. Sci.* **947**, 7-16.

Farge, M. & Rabreau, G. 1988 Transformée en ondelettes pour détecter et analyser les structures cohérentes dans les écoulements turbulents bidimensionnels. *C.R. Acad. Sci. Paris Série II* **307**, 1479-1486.

Farge, M. 1992 Wavelet transforms and their applications to turbulence. *Ann. Rev. Fluid Mech.* **24**, 395-457.

Frisch, U. 1995 *Turbulence.* Cambridge Univ. Press, Cambridge.

Gao H. & Ayyaswamy P.S. & Ducheyne P. 1997 Dynamics of a microcarrier particle in the simulated microgravity environment of a rotating-wall vessel. *Microgravity Sci. Technol.* **10(3)**, 154-165.

Gharib, M. & Kremers, D. & Koochesfahani, M.M. & Kemp, M. 2002 Leonardo's vision of flow visualization. *Experiments in Fluids.* **33**, 219-223.

Goupillaud, P. & Grossmann, A. & Morlet, J. 1984 Cycle-octave and related transforms in seismic signal analysis. *Geoexploration.* **23(1)**, 85-102.

Haase, M. 2000 Extracting singularities in turbulent flow with real and complex wavelets. In *Proceedings of the Science and Art Symposium 2000.* Eds A. Gyr, P.D. Koumoutsakos and U. Burr. Kluwer Academic Publishers, 1-11.

Hino, M. & Kashiwayanagi, M. & Nakayama, A. & Hara, T. 1983 Experiments on the turbulence statistics and the structure of a reciprocating flow. *J. Fluid Mech.* **131**, 63.

Jaffard, S. 1997 Multifractal Formalism for Functions Part I: Results Valid For All Functions. *SIAM Journal on Mathematical Analysis.* **28(4)**, 944 - 970.

Johari, H. & Durgin, W.W. 1998 Direct measurement of circulation using ultrasound. *Experiments in Fluids.* **25**, 445-454.

Kailas, S.V. & Narasimha, R. 1999 The eduction of structures from flow imagery using wavelets Part I. The mixing layer. *Experiments in Fluids.* **27**, 167-174.

Ku, D.N. & Giddens, D.P. & Zarins, C.K. & Glagov, S. 1985 Pulsatile flow and atherosclerosis in the human carotid bifurcation. Positive correlation between plaque location and low and oscillating shear stress. *Arteriosclerosis.* **5**, 293-301.

Ku, D.N. 1997 Blood flow in arteries. *Annu. Rev. Fluid Mech.* **29**, 399-343; *Atherosclerosis* **5**, 289-302.

Lin D.C, & Hughson R.L. 2001 Modeling heart rate variability in healthy humans: a turbulence analogy. *Phys. Rev. Lett.* **86(8)**, 1650-1653.

Mallat, S. & Hwang, W.L. 1992 Singularity detection and processing with wavelets. *IEEE Trans. Image Proc.* **38(2)**, 617-643.

Mallat, S. 1998 A wavelet tour of signal processing. Academic Press, San Diego.

Mantegna, R.N. & Stanley, H.E. 2000 *An introduction to Econophysics.* Cambridge Univ. Press, Cambridge.

May, P. & Gerbault, O. & Arrouvel, C. & Revol, M. & Servant, J.M. & Vicaut, E. 2001 Nonlinear analysis of arterial oscillated flow in experimental stenosis and microsurgical anastomosis. *J. Surg. Res.* **99(1)**, 53-60.

May, P. & Servant, J.M. & Vicaut, E. "Procédé d'analyse d'un événement tel qu'une intervention chirurgicale sur un vaisseau sanguin", French patent BRFR 0109145, 10 jully 2001. PCT/FR02/02419.

May, P. & Arrouvel, C. & Revol, M. & Servant, J.M. & Vicaut, E. 2002 Detection of hemodynamic turbulence in experimental stenosis: an in vivo study in the rat carotid artery. *J. Vasc. Res.* **39(1)**, 21-29.

Meneveau, C. 1991 Analysis of turbulence in the orthonormal wavelet representation. *J. Fluid Mech.* **232**, 469-520.

Muzy, J.F. & Bacry, E. & Arnéodo, A. 1991 Wavelets and multifractal formalism for singular signals: application to turbulence data. *Phys. Rev. Lett.* **67**, 3515-3518.

Muzy, J.F. & Bacry, E. & Arnéodo, A. 1994 The multifractal formalism revisited with wavelets. *Int. J. Bif. and Chaos.* **4**, 245-302.

Narasimha, R. & Saxena, V. & Kailas S.V. 2002 Coherent structures in plumes with and without off-source heating using wavelet analysis of flow imagery. *Experiments in Fluids.* **33**, 196-201.

Nerem, R.M. 1993 Hemodynamics and the Vascular Endothelium. *ASME Journal of Biomechanical Engineering.* **115**, 510-514.

Nowak, M. 2002 Wall shear stress measurement in a turbulent pipe flow using ultrasound Doppler velocimetry. *Experiments in Fluids.* **33**, 249-255.

Owsley, N.L. 2000 Array phonocardiography. In *Adaptive Systems for Signal Process-*

ing, Communications, and Control Symposium 2000. AS-SPCC. The IEEE 2000 , 31-36.

Peskin, C.S. & McQueen, D.M. 1995 A general method for the computer simulation of biological systems interacting with fluids. *Symp. Soc. Exp. Biol.* **49**, 265-276.

Radin, S. & Ducheyne, P. & Ayyaswamy, P.S. & Gao H. 2001 Surface transformation of bioactive glass in bioreactors simulating microgravity conditions. Part I: experimental study. *Biotechnol. Bioeng.* **75(3)**, 369-378.

Roshko, A. 1954 On the Development of turbulent wakes from vortex streets *NACA Report.* **1191**, 124-132.

Schmidt, D.W. & Tilmann, P.M. 1970 Experimental study of sound-wave phase fluctuations caused by turbulent wakes. *J. Acoustic. Soc. Am.* **47**, 1310-1324.

Spence, J.D. & Perkins, D.G. & Kline, R.L. & Adams, M.A. & Haust, M.D. 1984 Hemodynamic modification of aortic atherosclerosis. Effects of propranolol vs hydralazine in hypertensive hyperlipidemic rabbits. *Atherosclerosis.* **50(3)**, 325-333.

Tsao, P.S. & Buitrago, R. & Chan, J.R. & Cooke, J.P. 1996 Fluid flow inhibits endothelial adhesiveness. Nitric oxide and transcriptional regulation of VCAM-1. *Circulation* **94(7)**, 1682-1689.

Webster, D.R. & DeGraaff, D.B. & Eaton, J.K. 1996 Turbulence characteristics of a boundary layer over a two-dimensional bump. *J. Fluid Mech.* **320**, 53-69.

West, B.J. 1990 Physiology in fractal dimension: error tolerance. *Annals of Biomedical Engineering.* **18**, 135-149.

Winter, D.C. & Nerem, R.M. 1984 Turbulence in pulsatile flows. *Annals of Biomedical Engineering.* **12**, 357-369.

Witkin, A. 1983 Scale space filtering. In *Proc. Int. Joint. Conf. Artificial. Intell.* Espoo, Finland, 1983.

Ye, T. & Mittal, R. & Udaykumar, H.S. & Shyy, W. 1999 An Accurate Cartesian Grid Method for Viscous Incompressible Flows with Complex Immersed Boundaries. *Journal of Computational Physics* **156**, 209-240.